International Journal of Mechanics and Energy (IJME)
Vol. 1, Issue 2, 2013, ISSN: 2286-5845

MIXED CONVECTION FLOW IN THREE DIMENSIONAL LID-DRIVEN SQUARE CAVITY WITH VERTICAL TEMPERATURE GRADIENT

Noura BEN MANSOUR*, Nader BEN-CHEIKH, Brahim BEN-BEYA and Taieb LILI

* *Laboratory of Fluid Dynamics, Physics Department, Faculty of Sciences of Tunis,Campus Universitaire, 2092 El-Manar II, Tunisia.*

Abstract - In this study, the mixed convective heat transfer in a lid driven cubic cavity at is investigated numerically. Two cases are negotiated, the top moving lid and the bottom walls are at constant uniform temperatures (case 1: $T_{top} > T_b$, case 2: $T_{top} < T_b$) while the vertical walls are thermally insulated. The Reynolds number is fixed at Re=100, while the Richardson number is varied from 0.001 to 10. The effect of temperature gradient orientation on the fluid flow and heat transfer has been performed. It is shown that the downward temperature gradient yields a better heat transfer rate than the upward temperature gradients (case 1). Multiple correlations in terms of the heat transfer rate and Richardson number has been established.

Keywords - Mixed convection, Richardson number, lid-driven cavity, temperature gradients.

1. Introduction

In recent years the mixed convection in rectangular or square cavities has been investigated by many researchers. This attempt is due to the fact that heat transfer in a cavity can be found in many industrial and engineering applications such as electronic component cooling, food drying process, nuclear reactors etc… Flow and heat transfer phenomena caused by buoyancy and shear forces in enclosures have been studied extensively in the literature. For example, Iwatsu and Hyun [1] studied numerically three dimensional flows in cubical containers. The top moving wall is maintained at a higher temperature than the bottom wall. Numerical solutions are obtained over a wide range of physical parameters, $10^2 \leq \text{Re} \leq 2\times10^3$, $0 \leq \text{Ri} \leq 10$ and Pr = 0.71.

Numerical flow visualizations demonstrate the explicit effects of Ri as well as Re. Mohamed and Viskanta [2] investigated the effects of a sliding lid on the fluid flow and thermal structures in a lid-driven cavity. Moallemi and Jang [3] studied numerically mixed convective flows in a bottom heated square lid-driven enclosure. They investigated the effect of Prandtl number on the flow and heat transfer process. They found that the effects of buoyancy are more pronounced for higher values of Prandtl numbers, and they also derived a correlation for the average Nusselt number in terms of the Prandtl number, Reynolds number and Richardson number. Prasad and Koseff [4] performed an experimental investigation of mixed convection flow in a lid-driven cavity for different Richardson numbers, ranging from 0.1 to 1000. Their results indicate that the overall heat transfer rate is a

* **Corresponding author**: Noura Ben Mansour
E-mail: benmansournoura@yahoo.fr

very weak function of the Grashof number for the examined range of Reynolds numbers. They have also analyzed the mean heat flux values over the entire boundary to produce Nusselt number and Stanton number correlations which are very useful for design applications. Sharif [5] performed a numerical investigation with supplementary flow visualization of laminar mixed convective heat transfer in two-dimensional shallow rectangular driven cavities of aspect ratio 10. The top moving plate of the cavity is set at a higher temperature than the bottom stationary plate. Computations are reported for Rayleigh numbers ranging from 10^5 to 10^7 while keeping the Reynolds number fixed at 408.21, thus encompassing the wide spectrum of dominating forced convection, mixed convection, and dominating natural convection flow regimes. The fluid Prandtl number is taken as 6, representative of water. The effects of inclination of such a cavity on the flow and thermal fields are also investigated for inclination angles ranging from 0° to 30°. The author observed that the local Nusselt number at the heated moving plate starts with a high value and decreases rapidly to a small value towards the right side. The local Nusselt number at the cold plate reveals an oscillatory behavior near the right side due to the presence of a separation bubble at the cold surface in that location.

In the present work, the effect of temperature gradient orientation on the fluid flow and heat transfer in a lid-driven square cavity is investigated numerically.

2. Mathematical formulation

2.1 Governing equations

For laminar, incompressible and three-dimensional mixed convection, after invoking the Boussinesq approximation and neglecting the viscous dissipation, can be expressed in the dimensionless form as:

Continuity equation:

$$\frac{\partial u_i}{\partial x_i} = 0 \tag{1}$$

Momentum equations:

$$\left.\begin{aligned}
&\frac{\partial u}{\partial t}+\frac{\partial uu}{\partial x}+\frac{\partial uv}{\partial y}+\frac{\partial uw}{\partial z}=-\frac{\partial P}{\partial x}+\frac{1}{\mathrm{Re}}\left(\frac{\partial^2 u}{\partial x^2}+\frac{\partial^2 u}{\partial y^2}+\frac{\partial^2 u}{\partial z^2}\right)\\
&\frac{\partial v}{\partial t}+\frac{\partial uv}{\partial x}+\frac{\partial vv}{\partial y}+\frac{\partial vw}{\partial z}=-\frac{\partial P}{\partial y}+\frac{1}{\mathrm{Re}}\left(\frac{\partial^2 v}{\partial x^2}+\frac{\partial^2 v}{\partial y^2}+\frac{\partial^2 v}{\partial z^2}\right)\\
&\frac{\partial w}{\partial t}+\frac{\partial wu}{\partial x}+\frac{\partial wv}{\partial y}+\frac{\partial ww}{\partial z}=-\frac{\partial P}{\partial z}\\
&\qquad\qquad+\frac{1}{\mathrm{Re}}\left(\frac{\partial^2 w}{\partial x^2}+\frac{\partial^2 w}{\partial y^2}+\frac{\partial^2 w}{\partial z^2}\right)+Ri\theta
\end{aligned}\right\} \tag{2}$$

Energy equation:

$$\frac{\partial \theta}{\partial t}+\frac{\partial\left(u_i\theta\right)}{\partial x_i}=\frac{1}{\mathrm{Re}\,\mathrm{Pr}}\left(\frac{\partial^2\theta}{\partial x_i \partial x_i}\right) \tag{3}$$

Where, u, v and w are the velocity components in the x, y and z directions, respectively, θ is the temperature and P is the pressure. ρ is the density and g is the gravitational acceleration. In Eq. (2), the symbol δ_{i3} stands for the Krönecker delta. The chosen scales in Eqs. (1) – (3) are the length H, the velocity $u_0=\sqrt{g\beta H\Delta T}$, the time $t_0=\frac{H}{u_0}$ and the pressure $P_0=\rho u_0^2$. Further, the non-dimensional temperature is defined by $\theta=\left(T-T_r\right)\left(T_{hot}-T_{cold}\right)$, where the reference temperature is $T_r=\frac{\left(T_{hot}+T_{cold}\right)}{2}$. The non-dimensional numbers seen above, Gr, Re, Pr and Ri are the Grashof number, Reynolds number, Prandtl number and Richardson number, respectively, and they are defined as:

$Gr=\frac{g\beta\Delta TH^3}{\nu^2}$, $\mathrm{Re}=\frac{u_0H}{\nu}$, $\mathrm{Pr}=\frac{\nu}{\alpha}$ and $Ri=\frac{Gr}{\mathrm{Re}^2}$.

2.2 Initial and Boundary conditions

No slip condition at bottom and side walls. The upper lid has a constant velocity, u_0. The upper lid wall has an isothermal condition with temperature, $T=T_H$. The bottom wall is at rest and isotherm, i.e., $T=T_C$ ($T_C < T_H$). Finally, the remaining walls are adiabatic (see Fig.1).

2.3 Numerical procedure

Numerical computations were carried out with an in-house computer code written in the FORTRAN programming language.

In the FORTRAN code, the unsteady Navier–Stokes and energy equations are discretized by a second-order time stepping finite difference procedure. The procedure adopted here deserves a detailed explanation. First, the non-linear terms in Eqs. (2) are treated explicitly with a second-order Adams–Bashforth scheme. Second, the convective terms in Eq. (3) are treated semi implicitly. Third, the diffusion terms in Eqs. (2) and (3) are treated implicitly. In order to avoid the difficulty that the strong velocity-pressure coupling brings forward, we selected a projection method described in the work of Peyret and Taylor [6], Achdou and Guermond [7].

A finite-volume method is implemented to discretize the Navier–Stokes and energy equations (Patankar [8], Moukhalled and Darwish [9], Kobayachi and Pereira [10]). In this method, the solution domain is subdivided into small finite control volumes (CV). The grid used is more refined than that in areas in need and bigger in other zones.
In fact, it is necessary to use a fine mesh at the top and bottom wall, capable of accurately modeling the heat transfer and flow. With this approach, we can reduce the number of grid points without losing accuracy of calculation.

The advective terms in Eqs. (2) are discretized using a QUICK third-order scheme whereas a second-order central differencing (Hayase, Humphrey and Greif [11]) is applied in Eq. (3). The discretized momentum and energy equations are solved employing the red and black successive over relaxation method (RBSOR) [12], while the Poisson pressure correction equation is solved utilizing a full multi-grid method (Hortmann, Peric and Scheuerer [13], M.S. Mesquita and M.J.S. de Lemos [14], E. Nobile [15]). If specific details about the computational methodology are needed, the reader is directed to Ben-Cheikh et al. [16]. Finally, the convergence of solutions is assumed when the relative error for each variable between consecutive iterations is recorded below the convergence criterion ε such that:

$$\sum_{i,j,k}\left|\phi_{ijk}^{m+1}-\phi_{ijk}^{m}\right|\le\varepsilon$$

Here, ϕ represents a dependent variable u, v, w, or θ, the indexes i, j, k indicate a grid point, and the index m is the current iteration at the grid level. The convergence criterion was set to 10^{-6}.

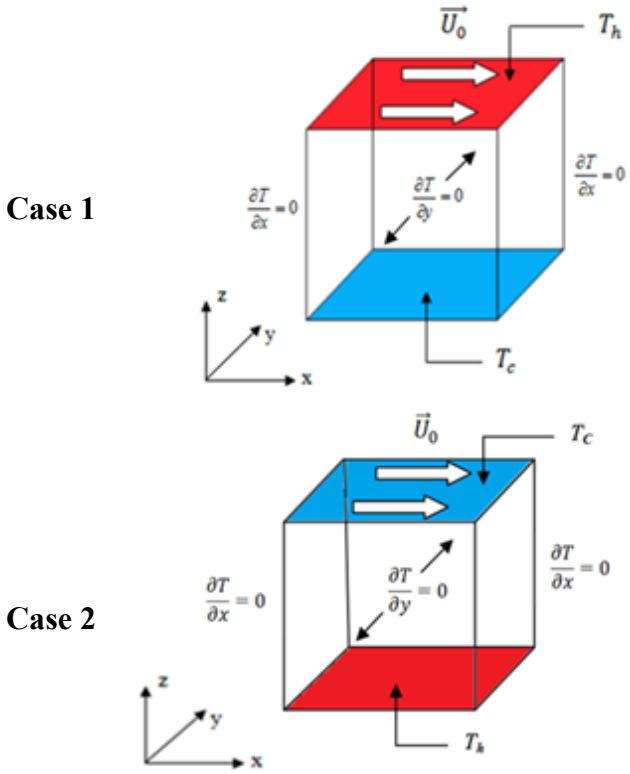

Fig.1: Physical model and boundary conditions for two cases.

3. Code validation

Table 1 Grid independency results for Re = 100, γ = 0°

	Ri=0.001		Ri=1		Ri=10	
Grid	48^3	64^3	48^3	64^3	48^3	64^3
Nusselt number	1.8371	1.8367	1.3487	1.3487	1.0927	1.0928

Table 2 Comparison of the computed average Nusselt number at the top wall.

Re	Ri=0.001			Ri=1			Ri=10		
	Ref[1]	Ref[17]	Pres.work	Ref[1]	Ref[17]	Pres.work	Ref[1]	Ref[17]	Pres.work
100	1.82	1.836	1.836	1.33	1.348	1.348	1.08	1.092	1.092
400	3.99	3.964	3.963	1.50	1.528	1.539	1.17	1.130	1.152
1000	7.03	7.284	7.295	1.80	1.856	1.863	1.37	1.143	1.143

The present numerical code is validated against a documented numerical study. Namely, the numerical solution reported by Iwatsu and Hyun [1]. The findings of the comparisons are documented in Table 2 for the average Nusselt number. The comparisons illustrate close proximity in the predictions made between the various solutions. These validation cases boost up the confidence in the numerical outcome of the present work.

The effect of grid resolution was also examined in order to select the appropriate grid density. Table 1 presents the results of a grid independency study showing the effects of number of grid points on Nusselt. A 48^3 non uniform grid is found to meet the requirements of both the grid independency study and the computational time costs.

4. Results and discussion

The effects of temperature gradient orientation on the steady state streamline, temperature, and Nusselt number are presented in the subsequent sections for three Richardson numbers. The Richardson number provides a measure for the relative importance of the thermal natural convection to the lid driven forced convection effect. The Richardson number is varied from 0.001 to 10 while Reynolds number is fixed at Re = 100. This variation gives transition from the natural convection dominated to forced convection dominated regimes.

4.1 Upward and downward temperature gradients

The influence of the upward temperature gradient (case1) on the transport phenomena is shown in Fig. 2 for Ri = 0.001, 1, and 10. For Ri = 10, the flow patterns are characterized by three primary recirculating counter-rotating vortices. This yields the stable stratification of temperature distribution as seen in subfigure 2c. The distribution of isotherms basically implies that the cavity is in a quasi-conduction domain, i.e., most of the heat transfer occurs due to conduction except that near the sliding top wall. As Ri is decreased to 1 (subfigures 2b and 2e), the bottom cell becomes feeble and amalgamate with the upper adjacent cell to provide only two extensive counter rotating cells. When Ri is further decreased to 0.001 (subfigures 2a and 2d), the effect of the mechanically driven top lid dominates the entire cavity and generates a primary recirculating vortex.

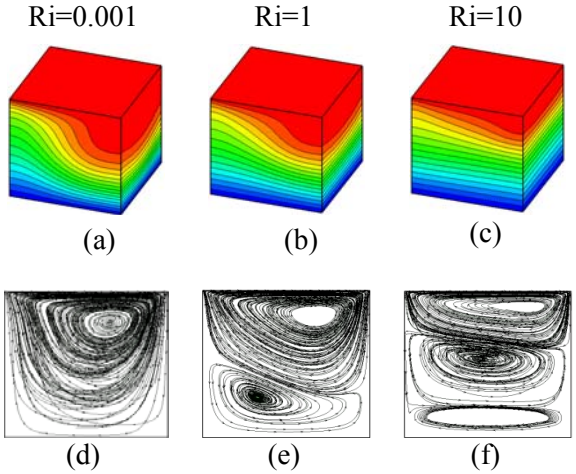

Fig.2. Computed isotherms (a,b and c) and streamlines (d,e and f) contours for case 1 and Ri = 0.001, 1 and 10.

The effect of the downward temperature gradient (case 2) on the streamline and isotherm patterns for Ri = 0.001, 1, and 10 is shown in Fig. 3. When Ri = 10, a single central primary vortex is observed covering the cavity domain. The vortex is driven by the moving lid. From subfigure 3c. the isotherms are symmetrical and clamped in the lower part of the plane (YOZ) and also we observed the appearance of the plume is believed to be the reason for the more enhancements in heat transfer.

The temperature and flow fields in the cavity for Ri = 1 are presented in subfigures 3b and 3e. It can be seen that the distribution of streamlines for Ri = 1 is similar to that of Ri = 10. When Ri is further decreased to 0.001 (subfigures 3a and 3d), the effect of the mechanically driven top lid, which is similar to case 1 with Ri=0.001, dominates the entire cavity and generates a primary recirculating vortex which was observed for the other Richardson number.

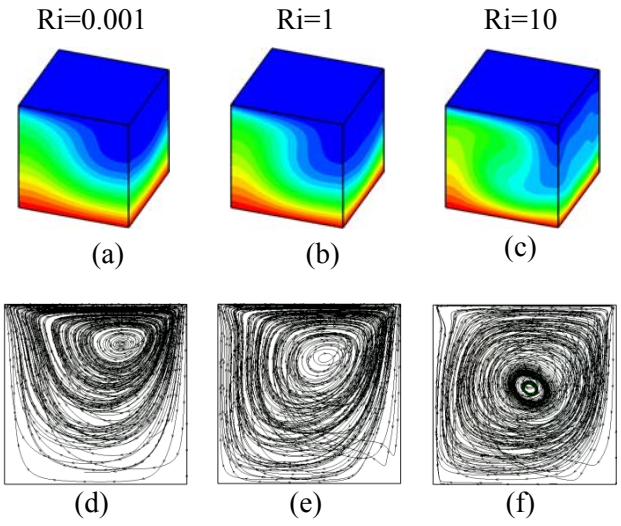

Fig.3. Computed isotherms (a,b and c) and streamlines (d, e and f) contours for case 2 and Ri=0.001, 1 and10.

Comparisons of the computed temperature and flow patterns, as shown in Figs. 2 and 3, reveal that the characteristics of mixed convection flow exhibit strong dependence on the orientation of the temperature gradients. For the upward temperature gradient (case 1), the flow possesses three recirculating vortices and the number of vortex decreases with decreasing Ri. The temperature distribution exhibits a vertical stratification. Whereas for the downward temperature gradient (case 2), the flow patterns show only one vortex dominates the entire cavity. The values of temperatures in the bulk region of the cavity are different for different orientations of temperature gradients.

4.2 Heat transfer rate and correlation

To examine the effects of temperature gradient orientation on heat transfer in the cavity, the average Nusselt number along the hot wall for different values of Ri as shown in Figs.4 and 5. For the upward temperature gradient (case 1) as shown in Fig. 4, the heat transfer rate of the top wall generally drops with lowering of Richardson number.

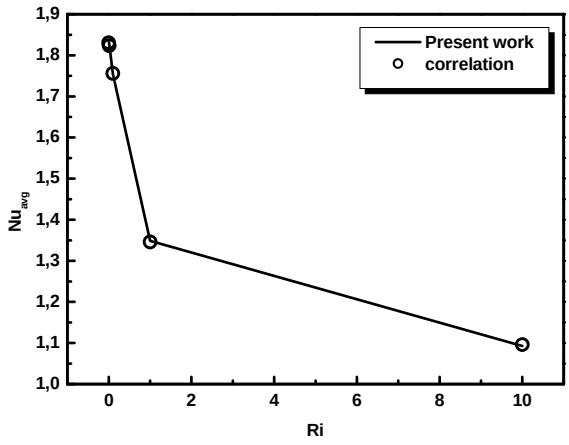

Fig. 4: Average Nusselt number along the hot wall for Re=100 (case 1).

For the downward temperature gradient (case 2) as shown in Fig. 5, the average heat transfer rate increase with the Richardson number. The downward temperature gradient (case 2) yields a better heat transfer rate than the upward temperature gradients (case 1) due to the increased buoyancy effects in the lower portions of the cavity. Referring to the literature

[18], multiple correlations in terms of the heat transfer rate and Richardson number has been established.

The average Nusselt number along the heated wall is correlated in term of Richardson number ($0.001 \leq Ri \leq 10$) for the two investigated cases. Using the numerical results, the correlation can be expressed as:

$Nu_{avg}=0.7353 \times 0.34^{Ri} +1.096$ **(Case 1)**

$Nu_{avg}=2.243 \times \log (2.204+Ri^{0.64})$ **(Case 2)**

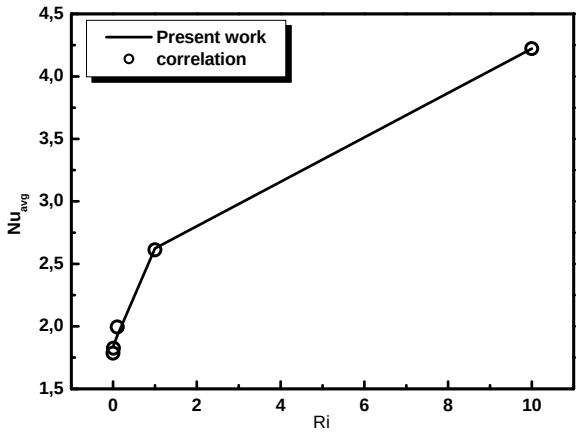

Fig. 5: Average Nusselt number along the hot surface for Re=100 (case 2).

Comparisons of the average Nusselt number between the numerical results and those obtained by the correlation are reported in Figs.4 and 5. As a result, the average Nusselt number computed from the above equations together with the numerical results agree well.

5. Conclusion

Numerical simulations of mixed convection in a lid-driven square cavity are made to investigate the effects of temperature gradient orientation on the flow field and heat transfer characteristics for five different values of the Richardson number ($Ri = 0.001 \leq Ri \leq 10$). Two different directions, namely, upward and downward temperature gradients, are considered in the present study. From the numerical results, the following conclusions may be drawn:

Case 1: When large Ri is united with Re= 100, three primary vortices are observed circumscribed in the proximity of the hot and cold walls and their intensity and their number are modified when Ri decreased. The rate of heat transfer to this case decreases with the Richardson number. A correlation in terms of the heat transfer rate and Richardson number has been established.

Case 2: When large Ri is united with low Re, a single central primary vortex is observed covering the cavity domain. This vortex decreases slightly when Ri decreased. The rate of heat transfer increases with the Richardson number. A correlation in terms of the heat transfer rate and Richardson number has been established also in this case.

Numerical results demonstrate that the downward temperature gradient yields a better heat transfer rate than the upward temperature gradients (case 1) due to the increased buoyancy effects in the lower portion of the cavity.

References

[1] R. Iwatsu and J.M. Hyun, Three-dimensionel driven-cavity flows with a vertical temperature gradient.

[2] A.A.Mohamed, R.Viskanta, Flow and heat transfer in a lid-driven cavity filled with a stably stratified fluid, Appl.Math. Modelling 19 (1995) 465-472.

[3] M. K. Moallemi and K. S. Jang, Prandtl number effects on laminar mixed convection heat transfer in a lid-driven cavity, hf. J. Hear Mass Transfer. Vol. 35, No. 8, pp. 1881-1892, 1992.

[4] A. K. Prasad and J.R. Koseff, Combined forced and natural convection heat transfer in a deep lid-driven cavity flow, Int.J..Heat Fluid Flow, Vol.17, pp. 460-467, 1996;

[5] M.A.R.Sharif, Laminar mixed convection in shallow inclined driven cavities with hot moving lid on top and cooled from bottom, Applied Thermal Engineering 27 (2007) 1036-1042.

[6] R. Peyret, T.D. Taylor, Computational Methods for Fluid Flow, Springer-Verlag, Berlin, Germany, 1983.

[7] Y. Achdou, J.L. Guermond, Convergence analysis of a finite element projection/Lagrange Galerkin method for the

incompressible Navier–Stokes equations, SIAM J. Numer. Anal. 37 (2000) 799–826.

[8] S.V.Patankar, A calculation procedure for two-dimensional elliptic situations, Numer. Heat Transfer 34 (1981) 409–425.

[9] F. Moukhalled, M. Darwish, A unified formulation of the segregated class of algorithm for fluid flow at all speeds, Numer. Heat Transfer, Part B: Fundamentals 37 (2000) 103–139.

[10] M.H. Kobayachi, J.M.C. Pereira, J.C.F. Pereira, A conservative finite-volume second-order-accurate projection method on hybrid unstructured grids, J. Comput. Phys. 150 (1999) 40–75.

[11] T. Hayase, J.A.C. Humphrey, R. Greif, A consistently formulated QUICK scheme for fast and stable convergence using finite-volume iterative calculation procedures, J. Comput. Phys. 98 (1992) 108 -118.

[12] W.H. Press, et al., second edition, Numerical Recipes in Fortran 77: The Art of Scientific Computing, vol. 1, Cambridge Press, London, UK, 1997.

[13] M. Hortmann, M. Peric, G. Scheuerer, Finite volume multigrid prediction of laminar natural convection: benchmark solutions, Int. J. Numer. Meth. Fluids 11 (1990) 189–207.

[14] M.S. Mesquita, M.J.S. de Lemos, Optimal multigrid solutions of dimensional convection–conduction problems, Appl. Math. Comput. 152 (2004) 725–742.

[15] E. Nobile, Simulation of time-dependent flow in cavities with the correction multigrid method, Part I: Mathematical formulation, Numer. Heat Transfer, Part B: Fundamentals 30 (1996) 341–350.

[16] N. Ben-Cheikh, B. Ben-Beya, T. Lili, Benchmark solution for time-dependent natural convection flows with an accelerated full-multigrid method, Num. Heat Trans. (B), 52 (2007) 131-151.

[17] Nasreddine Ouertatani, Nader Ben Cheikh,BrahimBenBeya ,TaiebLili, Antonio CampoMixed convection in a double lid-driven cubic cavity, Int. J.Therm.Sciences. Vol. 48, pp.1265–1272, 2009.

[18] Numerical Study of Mixed Convection Heat Transfer and Fluid Flow in Cubical Lid-Driven Cavity, Eur. J. Sci. Research, Vol.72 No.3 (2012), pp. 460-473.